Int. J. Electrochem. Sci., 13 **(2018)** 8072 – 8083, doi: 10.20964/2018.08.23

International Journal of ELECTROCHEMICAL SCIENCE
www.electrochemsci.org

Short Communication

The Inhibition Effect of 1-hydroxy-7-azabenzotriazole on X60 Pipeline Steel Corrosion in 1 M HCl Solution

Zhili Gong[1,2], *Shini Peng*[1,*], *Jie Chen*[1], *Lanzhou Gao*[1]

[1] School of Urban Construction and Environmental Engineering, Chongqing University, Chongqing 400044, China.
[2] School of Chemistry and Chemical Engineering, Yulin University, Yulin 719000, China.
[*]E-mail: psn2008@126.com; 2170200265@qq.com

Received: 13 April 2018 / *Accepted:* 17 May 2018 / *Published:* 5 July 2018

In this study, the effect of a benzotriazole derivative namely 1-hydroxy-7-azabenzotriazole (HOAT) on the inhibition of X60 pipeline steel corrosion in 1 M HCl solution was studied through complementary experimental approaches. Weight loss and electrochemical techniques including potentiodynamic polarization and electrochemical impedance spectroscopy (EIS), were employed to investigate the inhibition behavior of HOAT for steel corrosion. Weight loss analysis showed that inhibition efficiency of HOAT increases with its concentration and decreases with temperature. Electrochemical data provide good support to the weight loss study, and showed that HOAT behaves as a mixed-type corrosion inhibitor. Additionally, Langmuir adsorption model evidenced the adsorption of HOAT on the X60 steel surface via chemisorption mechanism.

Keywords: Corrosion Inhibition; X60 steel; EIS; AFM; Weight Loss.

1. INTRODUCTION

Mild steel is the most preferred material for industrial application because of its availability, low cost, and excellent physical properties [1, 2]. However, its application is restricted in acidic environments due to the susceptibility towards corrosion. One of the practical and cost effective approach to mitigate this problem is the use of corrosion inhibitors, which could form an effective barrier against corrosive species contained in the aqueous acidic media [3, 4]. Generally, corrosion inhibitors are organic molecules containing N, S, O, and P in their molecular structure which act as active centers for their interaction with metal surface [5-14]. The adsorption behavior could happened on the interface between the metal surface and corrosive media, which could denotes to the inhibition performance of the compound on this system.

The selection of proper molecules as effective corrosion inhibitors depends on their structure and formulation. However, the blind searching is still the main method to develop new effective corrosion inhibitors due to the unclear mechanism of inhibition. On account of this, the aim of this work is to understand the inhibition property of 1-hydroxy-7-azabenzotriazole (HOAT) shown in Fig. 1 against steel corrosion in acid solution and the inhibition mechanism. Therefore, the inhibition action of the HOAT for X60 pipeline steel have been investigated in 1 M HCl solution using measurements of potentiodynamic polarization, electrochemical impedance spectroscopy (EIS), weight loss, scanning electronic microscope (SEM), and atomic force microscope (AFM). Afterwards Langmuir adsorption model was used to interpret the inhibition mechanism of the investigated HOAT.

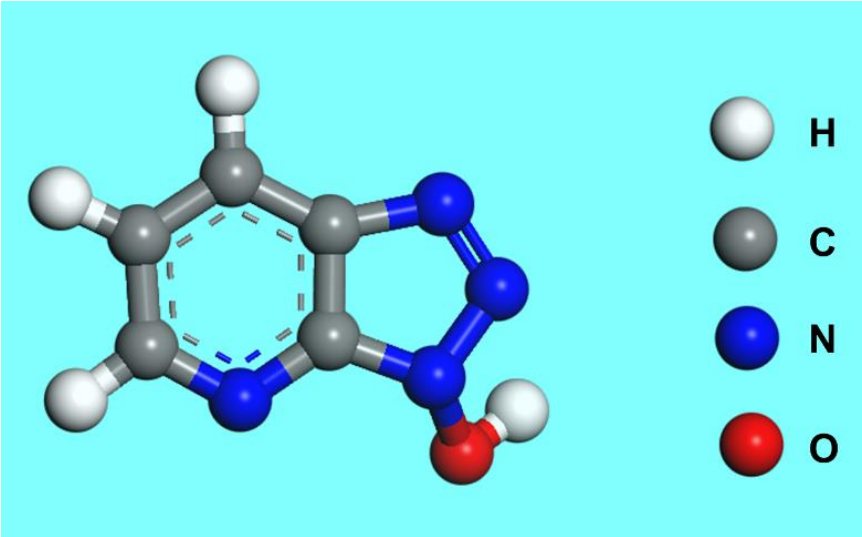

Figure 1. The molecular structure of HOAT.

2. EXPERIMENTAL

2.1. Sample and solution preparation

The composition (wt %) of the X60 steel specimen are as follows: C (0.124), Mn (1.73), Si (0.53), Cr (0.131), Cu (0.296), W (0.134), Ni (0.091), Mo (0.079), Sn (0.081), and remaining Fe. The steel was cut into coupons of 0.5 cm × 0.5 cm × 0.5 cm for surface analysis, 3 cm × 2 cm × 1 cm for weight loss test, and 1 cm × 1 cm × 1 cm for electrochemical experiment with an exposed area of 1 cm^2. Emery papers with 400-2000 grades were used to remove the oxide layer from the steel specimens. Then the specimens were degreased with ethanol, rinsed with deionized water, and dried in cold air. The corrosive medium was 1 M HCl prepared from 36% analytical grade reagents with deionized water. 1-hydroxy-7-azabenzotriazole (HOAT, Aladdin, 98%) was used as test inhibitor in the concentration range of 0.2–5 mM. In addition, the 1 M HCl solution in the absence of HOAT was taken as the blank for comparison.

2.2. Weight loss measurement

Some 500 mL glass beakers placed in a water thermostat were used to perform the weight loss test. The polished steel specimens were weighted and immersed in 1 M HCl solution with and without different concentrations of HOAT for 24 h in triplicate at 298-318 K, respectively. Then the X60 steel specimens were withdrawn, carefully rinsed with ultrapure water and acetone, then dried and weighted. The mean corrosion rates were finally calculated by immersion time and the weight loss of each specimen.

2.3. Electrochemical measurement

Electrochemical test was conducted to investigate inhibition ability of the inhibitor using CHI 660E electrochemical workstation in the conventional three-electrode system at 298K. Saturated calomel electrode (SCE) and Pt sheet (2.25 cm^2) were utilized as the reference electrode and the counter electrode, respectively. The X60 steel specimen was used as the working electrode. Prior each test, the open-circuit potential (OCP) measurement was carried out to reach a stable state. Then EIS was measured at the stable OCP. The range of frequency is between 10^5 Hz and 10^{-2} Hz and the signal amplitude is 5 mV. The EIS parameters were obtained by ZSimpWin software. Finally, the potentiodynamic polarization measurement was performed at ±250mV potential range versus the OCP with a scan rate of 1 mV/s.

2.4. Surface analysis

Field emission scanning electron microscope (FE-SEM) was applied to observe the surface morphology of X60 steel specimens after immersion in 1 M HCl solution with and without 5 mM HOAT for 6 h at 298 K. The surfaces of 1 h immersion were examined by atomic force microscope (AFM) using tapping mode.

3. RESULTS AND DISCUSSION

3.1. Weight loss study

The inhibition ability of HOAT at many concentrations on corrosion of X60 steel was studied by weight loss measurement at 298 K after 24 h immersion. The relevant corrosion rate (v, mg m^{-2} h^{-1}) and inhibition efficiency (η) are calculated as follows and shown in Fig. 2.

$$v = \frac{W_0 - W}{St} \quad (1)$$

$$\eta(\%) = \frac{v_0 - v}{v_0} \times 100 \quad (2)$$

where S is the total sample surface area, t is the immersion time, W_0 and W are the weight of samples before and after exposed to aggressive medium, respectively, v_0 and v are the corrosion rates of steel samples without and with HOAT, respectively.

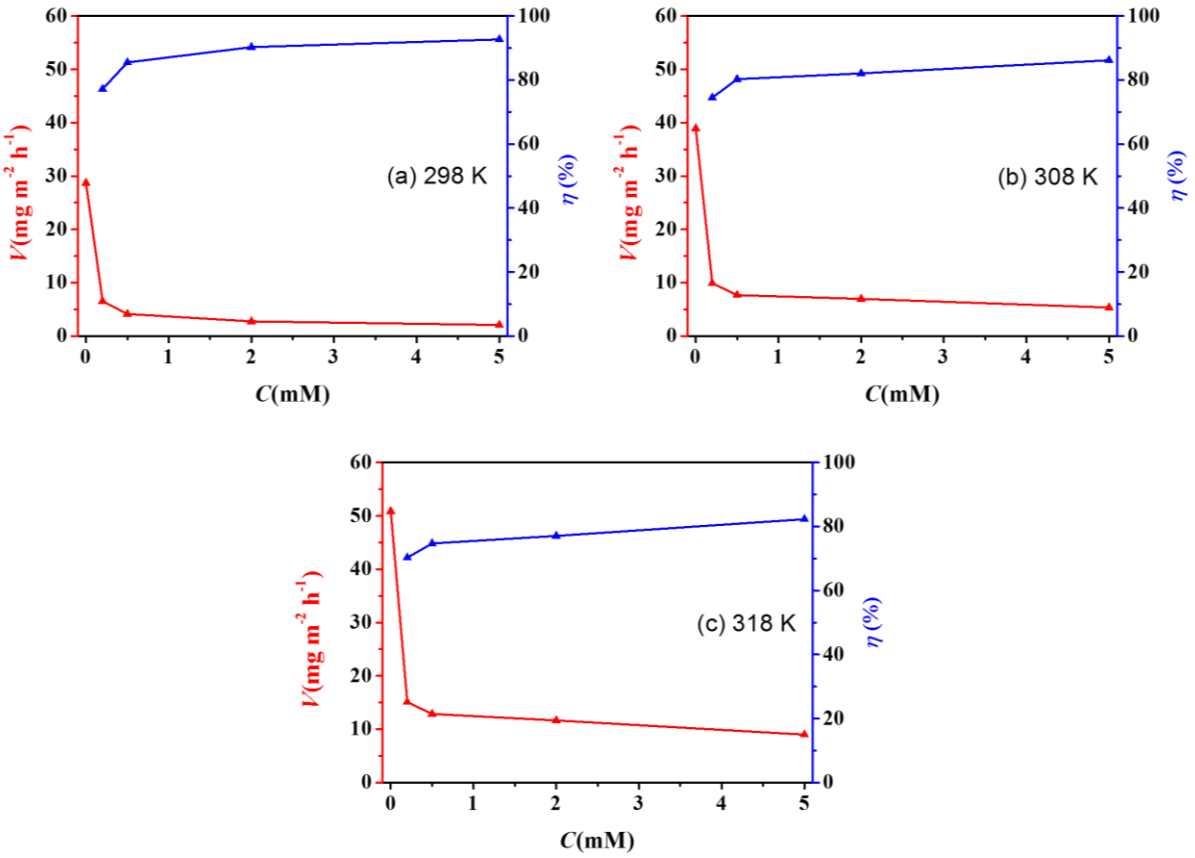

Figure 2. The weight loss graph for X60 steel in 1 M HCl solution without and with various concentrations of HOAT at (a) 298 K, (b) 308 K, (c) 318 K.

From results in Fig. 2, at each temperature, it can be seen that corrosion rates decrease and inhibition efficiencies increase with HOAT concentrations. Careful inspection of the results showed that values of the inhibition efficiency increase rapidly on increasing concentrations of HOAT from 0.2 mM to 0.5 mM. Whereas slight increase in the inhibition efficiencies obtained on enhancing its concentration from 0.5 mM to 5 mM. This observation indicates that at lower concentrations inhibition efficiencies enhance rapidly due to the substantial increase of the surface coverages. However, very little increases in the inhibition efficiency can be obtained after certain concentration when maximum surface (active sites) occupied by HOAT molecules, which could be contributed to intermolecular force repulsion causes irregular adsorption of the inhibitors molecules.

On the other hand, when the temperature increases, corrosion rates increase and therefore the corresponding inhibition efficiencies decrease, which indicates that the corrosion rate of steel is accelerated by rising the temperature. Fortunately, the inhibitor still showed high inhibitive ability at all temperatures, demonstrating that the corrosion reaction is significantly suppressed by HOAT. Especially, the maximum efficiencies are more than 90% at 298 K and 80% at 318 K, respectively.

3.2. Potentiodynamic polarization curves

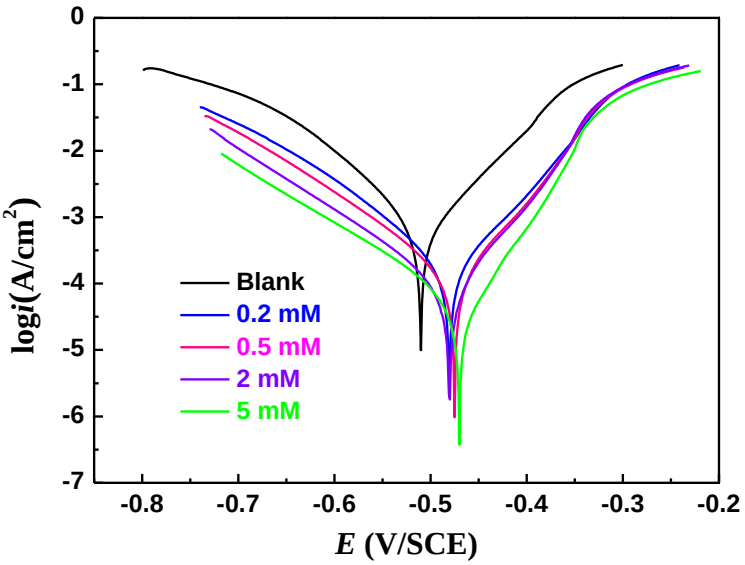

Figure 3. Polarization curves for X60 steel in 1 M HCl solution in the absence and presence of various concentrations of HOAT at 298K.

Fig. 3 shows potentiodynamic polarization curves recorded for X60 steel in 1 M HCl solution with and without various concentrations of the HOAT at 298 K. All electrochemical parameters are listed in Table 1. The i_{corr} is corrosion current density, the E_{corr} is corrosion potential, β_a and β_c are anodic and cathodic slope respectively. The inhibition efficiency η is defined as follows:

$$\eta(\%) = (1 - \frac{i_{corr}}{i_{corr,0}}) \times 100 \qquad (3)$$

where $i_{corr,0}$ and i_{corr} show current densities of steel electrode without and with the inhibitor in the 1 M HCl solution, respectively.

According to Fig. 3, it can be seen that in the presence of HOAT, the polarization curves shift obviously to lower current densities. This inhibition effect is increased vastly with increasing HOAT concentration. Besides, the cathodic and anodic part of polarization curve are both suppressed, indicating that HOAT reduces both cathodic hydrogen evolution and anodic steel dissolution to prevent steel from corrosion [15]. This situation shows that HOAT is a mixed-type inhibitor for steel corrosion [16]. Fig. 3 also demonstrates that the addition of HOAT does not change the values of slope, indicating that the inhibitor does not influence the reaction mechanism [17].

Table 1. Potentiodynamic polarization parameters for X60 steel with and without different concentrations of HOAT in 1 M HCl solution at 298 K.

C (mM)	E_{corr} (mV/SCE)	i_{corr} (μA cm^{-2})	β_c (mV dec^{-1})	β_a (mV dec^{-1})	η (%)
Blank	–510	608.3	–71.6	69.7	—
0.2	–481	155.6	–73.8	66.9	74.4

0.5	–475	106.4	–79.4	60.1	82.5
2	–480	77.9	–98.9	63.6	87.2
5	–470	38.0	–100.7	50.7	93.8

As seen in Table 1, the i_{corr} values decrease in the presence of HOAT and continue to reduce with increasing concentrations. As a result, the calculated inhibition efficiencies increase with incremental concentration of this inhibitor. The values of η reach up to 93.8% at 5 mM. This reveals that the formation of a protective film of HOAT on the X60 steel surface can defend the acid aggressive attack. Additionally, the obtained inhibition efficiencies agrees well with those calculated from weight loss test.

3.3. EIS measurement

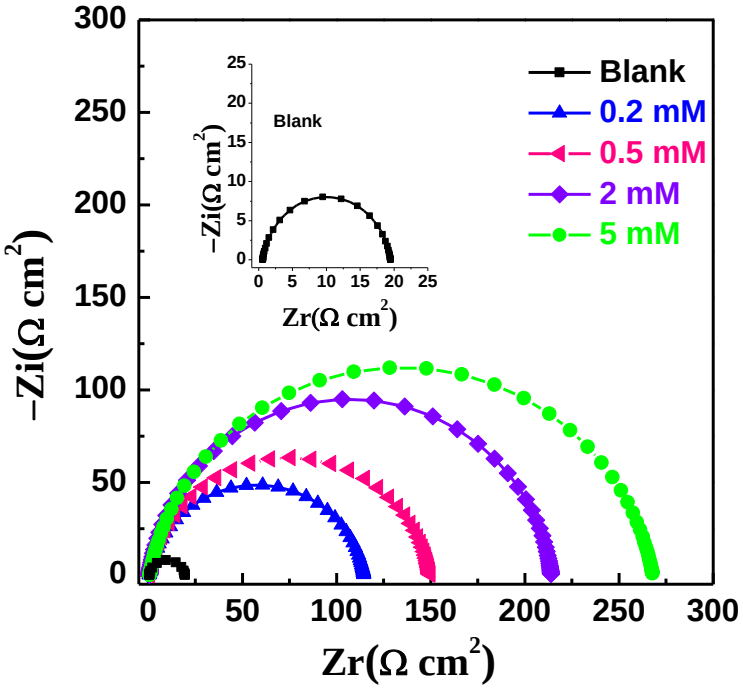

Figure 4. Nyquist curves of X60 steel in 1 M HCl solution in the absence and presence of different concentrations of HOAT at 298 K.

Nyquist plots for X60 steel specimens with and without various concentrations of HOAT in 1 M HCl are presented in Fig. 4. The single semicircle in the inhibited and non-inhibited steel are observed from Fig. 4, indicating that X60 steel corrosion with and without HOAT involves single charge transfer mechanism. In addition, it can be clearly seen that diameters of Nyquist plots of steel specimens increase with the addition and increase of HOAT as compared to the diameter of semicircles of uninhibited steel specimen, revealing that the corrosion of steel was effectively inhibited. However, the common properties and shapes of Nyquist plots of inhibited and uninhibited metallic specimens are similar, which indicates that HOAT molecules inhibit corrosion by enhancing the values of charge transfer resistance through their adsorption on steel surface [18].

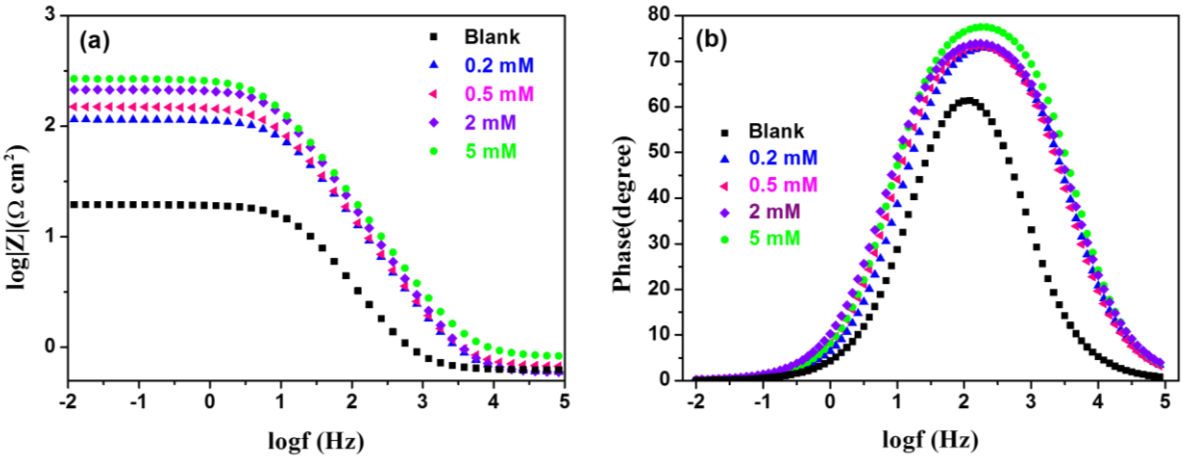

Figure 5. Bode plots for X60 steel electrode in 1 M HCl solution without and with different concentrations of HOAT at 298 K.

Fig. 5 shows the Bode plots. It is evident that the impedance values and frequency range with maximum phase become larger, accompanied with the rising HOAT concentration. This indicates that HOAT molecules gradually adsorb on the X60 steel substrate [19].

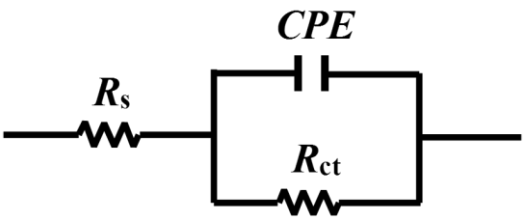

Figure 6. The equivalent circuit used for fitting the EIS data.

The equivalent electric circuit shown in Fig. 6 was used to fit the EIS data. R_s and R_{ct} are the solution and charge-transfer resistance, respectively, the *CPE* (constant phase angle elements constants) reflecting C_{dl} (double layer capacitance). The C_{dl} can be calculated as follows [20]:

$$C_{dl} = Y_0 \left(2\pi f_{max}\right)^{n-1} \quad (4)$$

where Y_0 is the magnitude of the *CPE*, f_{max} represents the frequency at the maximum value of the imaginary component in impedance spectra. n is the deviation parameter related to phase shift.

Table 2. Impedance parameters for X60 steel in 1 M HCl solution with and without of different concentrations of HOAT at 298 K.

C (mM)	R_s (Ω cm^2)	R_{ct} (Ω cm^2)	C_{dl} (μF cm^{-2})	n	η (%)
Blank	0.62	18.9	511.4	0.899	—
0.2	0.59	114	131.4	0.900	83.4

0.5	0.67	149	128.4	0.897	87.3
2	0.59	213	94.5	0.927	91.1
5	0.82	267	92.4	0.890	92.9

Table 2 shows the related impendence parameters. The inhibition efficiencies can be determined by,

$$\eta(\%) = (1 - \frac{R_{ct,0}}{R_{ct}}) \times 100 \quad (5)$$

From the results it can be seen that the values of R_{ct} are much higher for inhibited conditions as compared to the R_{ct} value of uninhibited condition, manifesting the HOAT-adsorption film on steel surface inhibites the charge transfer process. Whereas the values of C_{dl} display a decline tendency with the growing concentration of HOAT, which could be attributed to the gradually absorbed organic molecules, resulting to the decrease in the values of dielectric constants or due to increased thickness of electric double later films [21, 22]. The η value reached up to a high value of 92.9% at 5 mM HOAT from 83.4% at 0.2 mM HOAT. The inhibition efficiency values agree well with those obtained from weight loss and polarization tests.

3.4. Morphological observation

Fig. 7 shows the SEM images of X60 steel before and after immersed in 1 M HCl solution with and without 5 mM HOAT at 298 K. As seen in Fig. 7a, the steel surface is smooth only with some scratches, while steel surface is badly rough shown in Fig. 7b due to the attack from HCl solution. In the presence of the HOAT, the X60 steel surface in Fig. 7c is relatively smoother and less damaged or corroded, which can furtherly confirm the good inhibition action of HOAT for X60 steel in HCl solution.

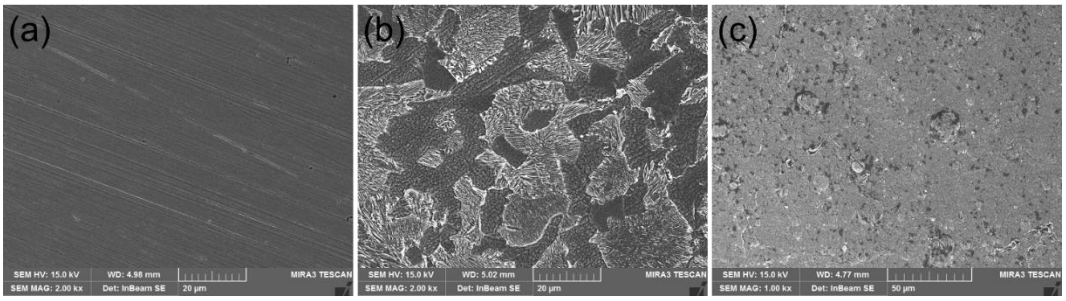

Figure 7. The X70 steel surface dipped in 1 M HCl solution, (a) polished surface, (b) corroded surface, (c) inhibited surface with 5 mM HOAT for 6 h at 298K.

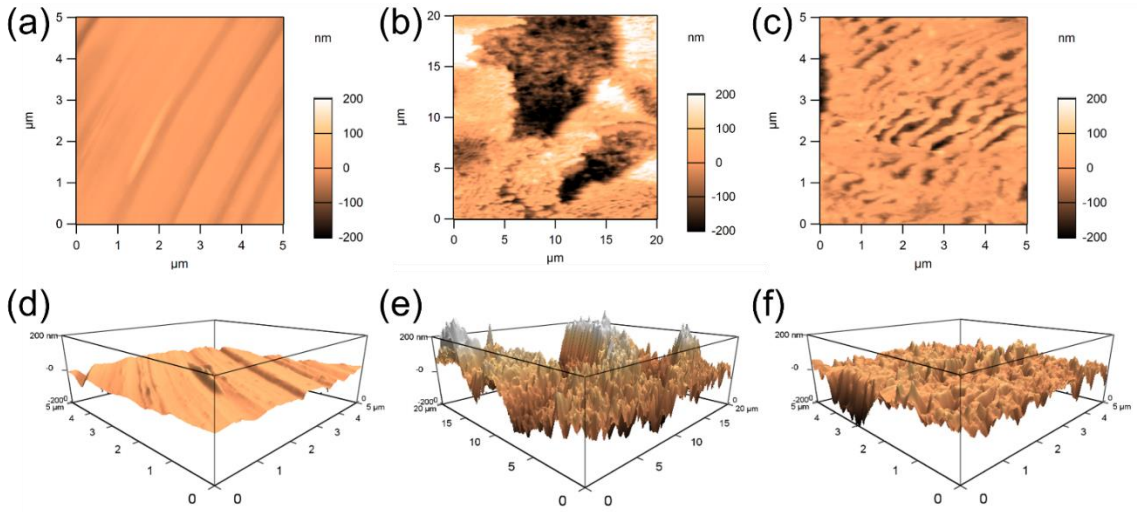

Figure 8. 2D AFM images of (a) polished steel, (b) corroded steel, (c) inhibited steel by 5 mM HOAT in 1 M HCl solution at 298 K for 1 h, 3D AFM images of (d) polished steel, (e) corroded steel, (f) inhibited steel by 5 mM HOAT in 1 M HCl solution at 298 K for 1 h.

AFM is also a powerful tool in corrosion field to observe surface appearance at the nano- to microscale level [23-25]. Fig. 8 presents the two-dimensional (2D), three-dimensional (3D) AFM images of polished, corroded and inhibited steel surfaces by 5 mM HOAT in 1 M HCl solution. As seen in Fig. 8(a, d) that the polished steel surface is smooth only with some small drapes. The calculated average surface roughness (R_a) of the surface was 8.58 nm. The corroded Cu sample shown in Fig. 8(b, e) is cracked considerably and exhibits rough structure with large and deep pits. However, with the addition of 5 mM HOAT, the relatively smoother and less damaged surface is obtained shown in Fig. 8(c, f), signifying that the corrosion rate of steel specimen remarkably decreases. Correspondingly, the calculated R_a values decreased from 86.26 nm (corroded surface) to 29.43 nm (inhibited surface).

3.5. Adsorption isotherm study

The interaction between the metal surface and organic inhibitor can be very well understood in terms of the adsorption isotherm. In this work, several classical adsorption isotherm models were used to fit the weight loss results [26, 27].

$$\frac{\theta}{1-\theta} = K_{ads}C \qquad \text{(Langmiur isotherm)} \quad (6)$$

$$(\frac{\theta}{1-\theta})\exp(2a\theta) = K_{ads}C \qquad \text{(Frumkin isotherm)} \quad (7)$$

$$\exp(-2a\theta) = K_{ads}C \qquad \text{(Temkin isotherm)} \quad (8)$$

where $\theta(\eta/100)$ is the coverage degree, C is the compound concentration, K_{ads} is the equilibrium constant of adsorption process.

As a result, Langmuir isotherm has a good linear relationship for the adsorption behavior of the investigated HOAT, with the linear regression coefficients (R^2) very close to 1. This indicates that

adsorption of HOAT on steel surface follows Langmuir adsorption model. As shown in Fig. 9(a-c), the relationship between *C* and *C/θ* complies straight lines with intercept of 1/*K*. The standard adsorption free energy (ΔG_{ads}^{0}) can be determined by [28, 29],

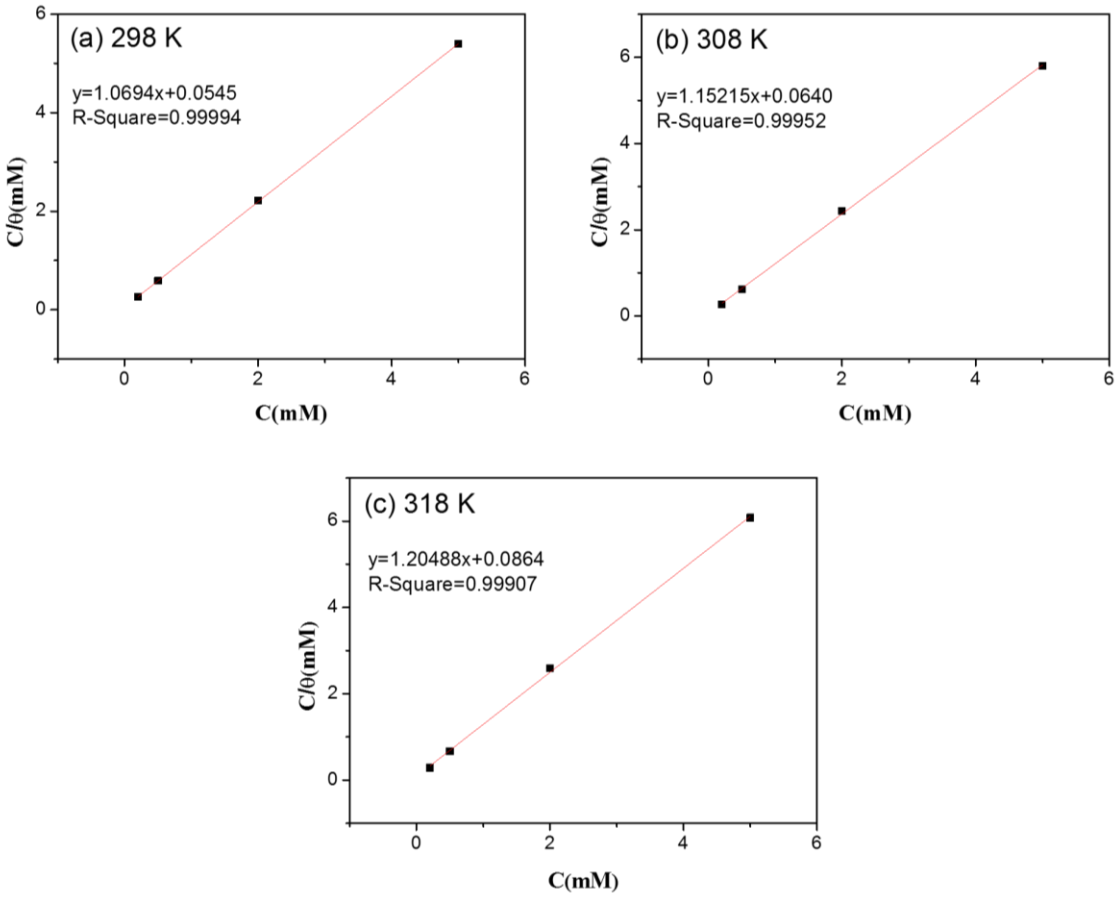

Figure 9. Langmuir isotherm model for HOAT on steel surface based on weight loss test.

$$\Delta G_{ads}^{0} = -RT\ln(55.5K_{ads}) \quad (9)$$

here, *T* (K) is the absolute temperature and *R* (8.314 J mol $^{-1}$ K $^{-1}$) is the molar gas constant.

The calculated values of ΔG_{ads}^{0} are −34.28 kJ/mol at 298 K, −33.87 kJ/mol at 308 K, −33.14 kJ/mol at 318 K, respectively. The negative sign of ΔG_{ads}^{0} indicates that the HOAT is spontaneously adsorbed onto the X60 steel surface [30]. As well known that the value of ΔG_{ads}^{0} around or lower than −40 kJ/mol can be deemed as chemisorption, which is due to the formation of covalent bond [31, 32]. If the ΔG_{ads}^{0} value is around or higher than −20 kJ/mol, it is assumed to physisorption. This is related to electrostatic interaction of charged metallic surface and inhibitor molecules [31, 32]. Therefore, it can be concluded that HOAT on steel surface in present study is mixed adsorption between physisorption and chemisorption.

4. CONCLUSIONS

In this study, the inhibition effect of HOAT on the X60 pipeline steel corrosion in 1 M HCl solution was studied through complementary experimental approaches, leading to the following conclusions:

(1) From weight loss experiment, the inhibition efficiency increases with the augment of HOAT concentration and decreases with raising the temperature. However, HOAT still exhibits favorable inhibition performance for the steel corrosion at high temperature.

(2) Electrochemical results indicates that HOAT is a mixed-type inhibitor and a HOAT-adsorption film is formed on steel surface. Moreover, the values of inhibition efficiency obtained from electrochemical tests are in good agreement with weight loss measurement.

(3) Surface observation confirmed the formation of a dense and ordered protective barrier on steel surface by HOAT, so that steel can be availably protected.

(4) HOAT adsorbs onto the steel surface chemically and physically to prevent the X60 steel corrosion. Besides, this adsorption is a spontaneous process, which follows Langmuir adsorption isotherm.

ACKNOWLEDGMENTS
We would like to thank the support from analysis and testing center of Chongqing University.

References

1. A. Dutta, S.K. Saha, U. Adhikari, P. Banerjee, D. Sukul, *Corros. Sci.*, 123 (2017) 256-266.
2. N. Kumari, P.K. Paul, L. Gope, M. Yadav, *J. Adhesion Sci. Tech.*, 31 (2016) 1524-1544.
3. G. Sığırcık, D. Yildirim, T. Tüken, *Corros. Sci.*, 120 (2017) 184-193.
4. E. Gutiérrez, J.A. Rodríguez, J. Cruz-Borbolla, J.G. Alvarado-Rodríguez, P. Thangarasu, *Corros. Sci.*, 108 (2016) 23-35.
5. H. Bi, G.T. Burstein, B.B. Rodriguez, G. Kawaley, *Corros. Sci.*, 102 (2016) 510-516.
6. K. Azzaoui, E. Mejdoubi, S. Jodeh, A. Lamhamdi, E. Rodriguez-Castellón, M. Algarra, A. Zarrouk, A. Errich, R. Salghi, H. Lgaz, *Corros. Sci.*, 129 (2017) 70-81.
7. L. Luo, S. Zhang, Y. Qiang, N. Chen, *Int. J. Electrochem. Sci.*, 11 (2016) 8177-8192.
8. N.X. Chen, S.T. Zhang, Y.J. Qiang, S.Y. Xu, X.L. Ren, *Int. J. Electrochem. Sci.*, 11 (2016) 7230-7241.
9. Y. Qiang, S. Zhang, S. Xu, W. Li, *J. Colloid Interf. Sci.*, 472 (2016) 52-59.
10. O. Olivares-Xometl, E. Álvarez-Álvarez, N.V. Likhanova, I.V. Lijanova, R.E. Hernández-Ramírez, P. Arellanes-Lozada, J.L. Varela-Caselis, *J. Adhesion Sci. Tech.*, 32 (2017) 1092-1113.
11. S.A. Umoren, A. Madhankumar, *J. Mol. Liq.*, 224 (2016) 72-82.
12. G.L.F. Mendonça, S.N. Costa, V.N. Freire, P.N.S. Casciano, A.N. Correia, P.d. Lima-Neto, *Corros. Sci.*, 115 (2017) 41-55.
13. Y. Qiang, S. Zhang, L. Guo, X. Zheng, B. Xiang, S. Chen, *Corros. Sci.*, 119 (2017) 68-78.
14. Y. Qiang, S. Zhang, B. Tan, S. Chen, *Corros. Sci.*, 133 (2018) 6-16.
15. G. Karthik, M. Sundaravadivelu, *J. Adhesion Sci. Tech.*, 31 (2016) 530-551.
16. Z. Tao, S. Zhang, W. Li, B. Hou, *Corros. Sci.*, 51 (2009) 2588-2595.
17. G. Khan, W.J. Basirun, S.N. Kazi, P. Ahmed, L. Magaji, S.M. Ahmed, G.M. Khan, M.A. Rehman, *J. Colloid Interf. Sci.*, 502 (2017) 134-145.

18. P. Singh, E.E. Ebenso, L.O. Olasunkanmi, I.B. Obot, M.A. Quraishi, *J. Phys. Chem. C*, 120 (2016) 3408-3419.
19. Y. Qiang, S. Zhang, S. Yan, X. Zou, S. Chen, *Corros. Sci.*, 126 (2017) 295-304.
20. A. Yousefi, S. Javadian, J. Neshati, *Ind. Eng. Chem. Res.*, 53 (2014) 5475-5489.
21. Y.J. Qiang, S.T. Zhang, S.Y. Xu, L.L. Yin, *RSC Adv.*, 5 (2015) 63866-63873.
22. J. Chen, Y. Qiang, S. Peng, Z. Gong, S. Zhang, L. Gao, B. Tan, S. L. Guo, *J. Adhesion Sci., Tech.*, 32 (2018) 2083-2098.
23. G. Ji, S. Anjum, S. Sundaram, R. Prakash, *Corros. Sci.*, 90 (2015) 107-117.
24. C. Verma, A. Singh, G. Pallikonda, M. Chakravarty, M.A. Quraishi, I. Bahadur, E.E. Ebenso, *J. Mol. Liq.*, 209 (2015) 306-319.
25. Y. Qiang, S. Zhang, L. Guo, S. Xu, L. Feng, I.B. Obot, S. Chen, *J. Clean. Prod.*, 152 (2017) 17-25.
26. Y. Qiang, S. Zhang, S. Xu, L. Guo, N. Chen, I.B. Obot, *Int. J. Electrochem. Sci.*, 11 (2016) 3147-3163.
27. M.B. Radovanović, M.M. Antonijević, *J. Adhesion Sci., Tech.*, 31 (2017) 369-387.
28. S.A. Umoren, Z.M. Gasem, I.B. Obot, *Ind. Eng. Chem. Res.*, 52 (2013) 14855-14865.
29. D.K. Yadav, M.A. Quraishi, *Ind. Eng. Chem. Res.*, 51 (2012) 14966-14979.
30. Sudheer, M.A. Quraishi, *Ind. Eng. Chem. Res.*, 53 (2014) 2851-2859.
31. A.O. Yüce, G. Kardaş, *Corros. Sci.*, 58 (2012) 86-94.
32. A.K. Singh, M.A. Quraishi, *Corros. Sci.*, 52 (2010) 152-160.